Paper awarded the international PIANC G. Willems Prize Competition, 2001

Experimental study and numerical modelling of pore pressure attenuation inside a rubble mound breakwater

Peter Troch
Post-Doctoral Research Assistant, Dept. of Civil Engineering,
Ghent University, Technologiepark 904, B-9052 Zwijnaarde (Belgium).
email: Peter.Troch@UGent.be, fax: +32 (0)9 264 58 37

Abstract

The main objective of this paper is to study the attenuation of the wave induced pore pressures inside the core of a rubble mound breakwater. The exact knowledge of the distribution and the attenuation of the pore pressures is very important for the design of a stable and safe breakwater. Until now no tools have been presented for the detailed determination of the pore pressures and the related porous flow field in the breakwater core. The pore pressure attenuation is studied using experimental data (in section 2) and using a numerical wave flume (in section 3).

The experimental study includes the analysis of prototype data from the Zeebrugge breakwater and large scale data from a physical breakwater model. Both data sets are presented. The Zeebrugge prototype data are unique world-wide and have not been analysed before. The large scale data are taken from literature and have been re-analysed in detail with respect to the attenuation characteristics. The conclusions from the analysis are compared and synthesised into a practical calculation method for the attenuation of the pore pressure heights in the breakwater core. This new calculation method is the most important result in this paper. The practical use for design applications is explained.

The attenuation of pore pressures in a breakwater core is also studied in the numerical wave flume VOFbreak^2. The validation of the numerical wave flume using physical model data is presented. The results from the numerical modelling of the wave interaction with the breakwater are compared to the results from the experimental study.

The work presented in this paper is a summary of the Ph.D. research of the author.

1 Introduction

Coastal zones typically have high densities of population, and important harbours with intense economic activities are located along the coastlines. Usually coastal structures, such as sea dikes, breakwaters, quay walls, jetties, etc… are constructed to protect people and harbour activities against waves and flooding. In this paper one type of coastal structure will be looked at in more detail: the rubble mound breakwater. Although the construction world-wide of such breakwaters results in large differences in used materials and in wave loads, yet it is possible to reduce the geometry and the materials into one typical design cross section (Fig. 1).

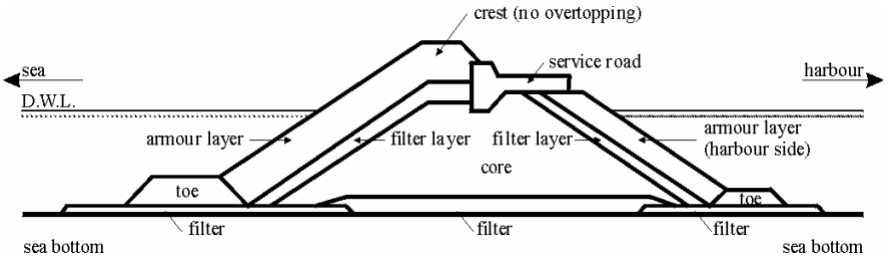

Fig. 1. *Typical cross section of a rubble mound breakwater (no overtopping conditions).*

The core is made of rock and constitutes the main part of the breakwater. The porous flow inside the permeable core is caused by the waves and experiences high energy dissipation due to friction losses. The core material itself is not stable under wave attack and is protected by an armour layer of individual heavy concrete blocks. These armour units withstand the waves. A toe at the sea bottom acts as a foundation for the armour layer. A filter layer between the core and the armour layer also acts as foundation layer for the armour layer, and prevents that the fine rock in the core is washed out in between the holes of the armour layer. A superstructure on top of the core allows access on the breakwater.

The interaction between the waves and the breakwater is described by a large number of related physical processes. As an example, the breakwater at Zeebrugge in Belgium is shown during storm conditions (Fig. 2). Waves propagate towards the breakwater and run up and down the armour layer. Part of the wave energy is reflected back to the sea, part of the energy is dissipated in the armour and filter layer and in the core, the remaining part is transmitted through the breakwater. The porous flow inside the core has both laminar and turbulent flow characteristics and is connected to the wave attack via infiltration and seepage through the armour layer. The hydrodynamic pore pressures associated with the porous flow (i.e. the wave induced water pressure inside the holes of the skeleton of the rock material) decrease with increasing distance from the seaward slope. In Allsop and Wood (1987) a comprehensive literature overview is made of all related hydrodynamic and geo-technical processes.

Fig. 2. *Photo of wave interaction with the Zeebrugge rubble mound breakwater during storm conditions (significant wave height estimated around 3 meters).*

This description of the interaction between waves and breakwater shows that it is not an easy task to formulate the governing physical processes accurately. Therefor the design of rubble mound breakwaters is mainly based on empirical relationships and on physical model results. A number of recent failures of rubble mound breakwaters during storms (e.g. Sines (Portugal) and Bilbao (Spain) in Europe, Tripoli (Libya) and Diablo Canyon (USA) outside Europe) proof that the present-day design methods should be improved.

Harlow (1980) reports some of the failures and concludes that in most cases the failure is caused by very large pore pressures in the breakwater core. De Groot et al. (1994) present the importance of the knowledge of the pore pressures in the design of a breakwater, in particular for the slope stability analysis, for the design of filter constructions near the bottom of the breakwater, and for the influence of pore pressures on hydraulic stability of armour units, on wave run-up and overtopping, on wave transmission and on internal set-up of the phreatic water table.

The exact knowledge of the pore pressures therefor is very important for a stable and safe breakwater structure. However it is very difficult to estimate the magnitude of the pore pressures accurately. Due to the complexity of both wave loads and structure itself there are no analytical expressions available. In conventional small scale model tests (scale ranging between 1:30 till 1:70) viscous scale effects influence the porous flow inside the breakwater core adversely. Moreover it is generally accepted (Price, 1983; Barends, 1986; Allsop and Wood, 1987; Thornton et al., 2000) that prototype data of pore pressures are the missing link in order to improve the understanding of the physical processes, en hence to improve the design process.

In this paper a calculation method will be presented for the determination of the pore pressures inside the breakwater core caused by wave attack. The relatively simple method is based on an experimental study of pore pressure attenuation using prototype data and large scale data. The prototype data have never been used before and are unique world-wide. The large scale data are taken from literature and are analysed in more detail for use in this paper. A numerical wave flume is extended in order to simulate wave-breakwater interaction and is validated using physical model data. The performance of the numerical modelling of the wave interaction with a breakwater is tested by comparing pore pressures in the core, determined from both the experimental study and the numerical modelling.

2 Experimental study of pore pressure attenuation

2.1 Theoretical background on attenuation of pore pressures

Theoretical work dealing with oscillatory flow in porous media was carried out by Biesel (1950) who identified the form of the spatial and temporal relationships which describe a linearly damped oscillatory flow. Le Méhauté (1958) applied this relationship to rubble mound breakwaters by introducing parameters accounting for porosity and inertia effects of the porous material. Oumeraci and Partenscky (1990) summarise Le Méhauté's theory on this topic and conclude that the height of the pore pressure oscillation $p(x)$ of a propagating pressure wave decreases exponentially with the distance to the breakwater interface according to the linear damping model:

$$p(x) = p_0 \exp(-\delta \frac{2\pi}{L'} x) \qquad (1)$$

where x is the co-ordinate across the core (m), where x = 0 at the interface between filter layer and core; $p(x)$ is the pore pressure height at position x (kPa); p_0 is the reference pore pressure height at x = 0 (kPa), L' is the wave length within the breakwater (m), δ is a damping coefficient (-). The wave length within the breakwater L' is calculated from $L' = L/\sqrt{1.4}$ (Oumeraci, 1991), where L is the wave length. The pore pressure height $p(x)$ is the envelope function of the instantaneous pore pressures $p(x,t)$ along the x-axis. From equation (1) it is clear that the attenuation of the pore pressure heights is exponential.

A number of important comments are formulated with regard to the linear damping model (1):

- There has not been reported any improved theoretical damping model since the 50's. Also no detailed experimental validation of the damping model (1) is reported in literature.

- The underlying friction model in (1) is described using only one linear term (i.e. friction is proportional to the velocity). This corresponds to the use of the well-know Darcy flow resistance where only viscous flow resistance is accounted for. In the case of porous flow in a rubble mound breakwater, there is also a large turbulent flow resistance present. In this latter case the friction model contains an additional non-linear term, and is called the Fochheimer model (Burcharth and Andersen, 1995). Later in this paper the application and validity of (1) will be verified.

- The linear damping model (1) is a one-dimensional representation of a two-dimensional problem since the damping is described only in horizontal direction. There is obviously also attenuation of pore pressure heights in vertical direction. Moreover the damping coefficient δ is defined as a constant, not as a function of distance along the vertical axis. In the experimental study this will be investigated in more detail.

2.2 Prototype pore pressure measurements at Zeebrugge breakwater

2.2.1 Description of Zeebrugge prototype monitoring system

At the Zeebrugge harbour (Belgium) a cross-section of the NW-breakwater has been instrumented for the study of physical processes related to the behaviour of a prototype rubble mound breakwater in random wave conditions. Within the EC MAST programme this monitoring system has been re-engineered and extended to a high-quality full scale data acquisition centre. The development of the prototype monitoring system to a world-wide unique system with respect to the infrastructure available at Zeebrugge, the instrumentation installed on site, and the data management developed, is briefly summarised here. For more detailed information on the prototype measurements, see Troch et al. (1998) or Troch (2000).

a. Infrastructure

The port of Zeebrugge is situated on the eastern part of the Belgian coastline, and is protected by two main breakwaters. The Zeebrugge breakwaters constitute of conventional rubble-mound breakwaters with a low superstructure and an armour layer consisting of grooved cubes (25 ton), see Fig. 3. The breakwater core consists of quarry run 2-300 kg, the filter layer is made of rock 1-3 ton. On the breakwater crest, a service road enables easy access of the breakwater. The tidal range at spring tide is 4.3 m.

A measurement jetty of 60 m length supported by a steel tube pile at the breakwater toe and by concrete columns on top of the breakwater is situated on the NW-breakwater, Fig. 3. Six bore-holes have been drilled in the core: four vertical bore-holes and two oblique bore-holes. Galvanised steel casings are placed in these bore-holes. These casings are perforated in order not to disturb the overall permeability. Pressure sensors are mounted in these casings. Each pressure sensor cable is protected by a high density polyethylene tube provided with a perforated nylon head at the sensor end.

In a container, placed on the landward side of the breakwater, signal conditioning apparatuses and a data acquisition system are installed. All electric cables from the measuring sensors are lead towards the container and the PC.

b. Instrumentation

An overview of instrumentation installed on the measurement jetty is given in Fig. 3, and summarised in Table 1.

Wave rider buoys are located in front of the breakwater and measure the incident waves. The water level at the toe of the breakwater is measured by an infra-red wave height meter and by two submerged pressure sensors located in front of the steel tube pile.

A set of vertically placed stepgauges between the measurement jetty and the armour layer is able to detect the wave run-up and run-down on the armour layer. A run-up gauge placed on top of the armour units is also used for wave run-up measurements.

Inside the core 13 pressure sensors are installed in the six bore-holes for the measurement of the internal pore pressures induced by the waves. Assembly of the sensors is conceived to allow flexible placement in the bore-holes, ease of maintenance and ease of calibration.

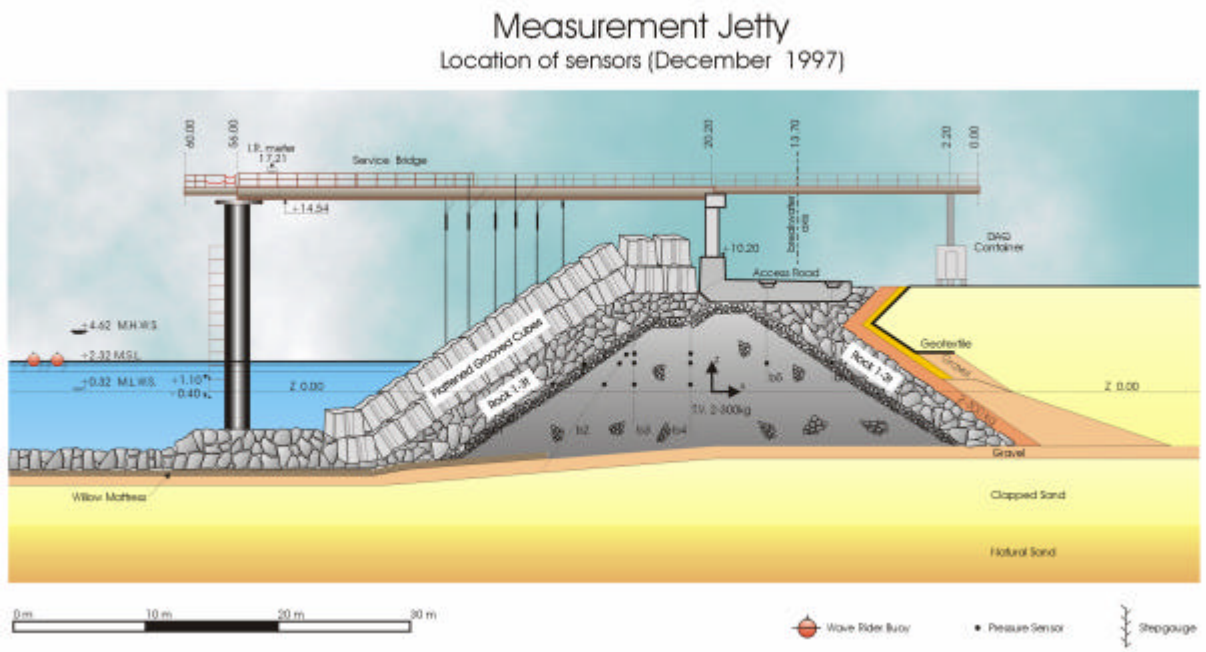

Fig. 3. *Zeebrugge breakwater: design cross section and prototype monitoring system with measurement jetty and location of instruments.*

Table 1. *Instrumentation installed on prototype monitoring system at Zeebrugge breakwater.*

INSTRUMENTATION	LOCATION	AIM OF MEASUREMENT
2 waverider buoys	150 m and 215 m from breakwater	wave records
infra-red wave height meter	near steel tube pile	wave records, tide level
2 submerged pressure sensors	near steel tube pile	wave records, tide level
5 vertically placed stepgauges	between armour layer and jetty beam	run-up/run-down wave profiles
1 run-up gauge (5 parts)	on one face of armour unit	run-up/run-down wave profiles
13 pressure sensors	inside rubble core	pressure records

c. Data Management

A strategic data management plan has been developed for acquisition, processing and distribution of all full scale data.

The on line data acquisition is done by using a PC with LabVIEW software and a National Instruments DAQ-board. The sample frequency is set to 10 Hz for all channels. Raw data are stored on the hard disk.

The off line data processing includes back-up of raw data on CD-ROM, data editing and quality control, and finally analysis and interpretation of the prototype measurements.

All data are collected in a prototype measurements database. Up to date about 16 storms with significant wave heights ranging between 1.00 m and 3.50 m, and wind directions from NW - allowing almost perpendicular wave attack- have been collected. Continuously improvements and new instruments are prepared and installed, keeping the prototype monitoring system highly operational. For more detailed information and technical details of instrumentation and data acquisition, the reader is referred to (Troch et al., 1996-a; Troch et al., 1996-b).

2.2.2 Analysis of Zeebrugge prototype pore pressure measurements

The main objective of a breakwater is to dissipate incident wave energy when waves propagate through the porous breakwater core. This points out the relevance of investigating the breakwater's capability in this respect. In this section, results from analysis of prototype measurements of pore pressure attenuation are presented.

a. Typical time series of prototype measurements

Fig. 4 shows a typical example of the time series and corresponding energy density spectra of a wave buoy (WR), the IR-meter (IR), and 4 consecutive pressure sensors (385, 386, 388 and 384 resp.) at the same level Z+2.40 m, for a storm that occurred on 04.11.1999. The wave buoy detects elevations (and wave heights derived from that) in front of the breakwater (distance about 200 m to slope), the IR-meter measures elevations at the breakwater toe, and the 4 pressure sensors show clearly the attenuation of the instantaneous pore pressures (and consequently the

attenuation of the pore pressure heights) inside the breakwater core. The significant pore pressure height p_s is calculated from

$$p_s = 4\sqrt{m_0} \tag{2}$$

where m_0 is the moment of order zero:

$$m_0 = \int_{\frac{1}{3}f_p}^{3f_p} S(f)\, df \tag{3}$$

and $f_p = 1/T_p$ is peak frequency, $S(f)$ is energy density spectrum of the pressure time series.

The spectral shape remains more or less constant, with constant peak period T_p = 7.1 s, and decreasing pore pressure heights p_s.

b. Determination of damping coefficient δ

The Zeebrugge prototype data set is used for the experimental analysis of the pressure wave attenuation in the breakwater core. The exponential damping model (1) will be used to describe the attenuation, here re-written as:

$$p_s(x') = p_{0,s} \exp(-\delta \frac{2\pi}{L'} x') \tag{4}$$

where x' is the horizontal distance between the pressure sensor positions, $p_s(x')$ is the significant pore pressure height derived from the pressure sensor at position x', and $p_{0,s}$ is the reference pore pressure height at the first pressure sensor closest to the interface between filter layer and core.

The prototype time series are split into 15 minutes wave and pressure records. It is assumed that wave and water level conditions remain constant during this short period of time. In Fig. 5 pressure heights $p_s(x')$ of 5 pressure sensors (385, 386, 381, 388 and 384 resp.) are plotted versus the horizontal distance x' inside the core, for the 15 minutes wave record from the typical example in Fig. 4. The exponential model (4) is fitted through the prototype data and a damping coefficient δ = 0.67 is obtained.

From Fig. 5 it is concluded that there is good agreement between the attenuation measured in prototype conditions and the theoretical exponential damping model (4). This shows that the damping model (4) is capable to predict pore pressure attenuation inside a breakwater core, governed by the damping coefficient δ.

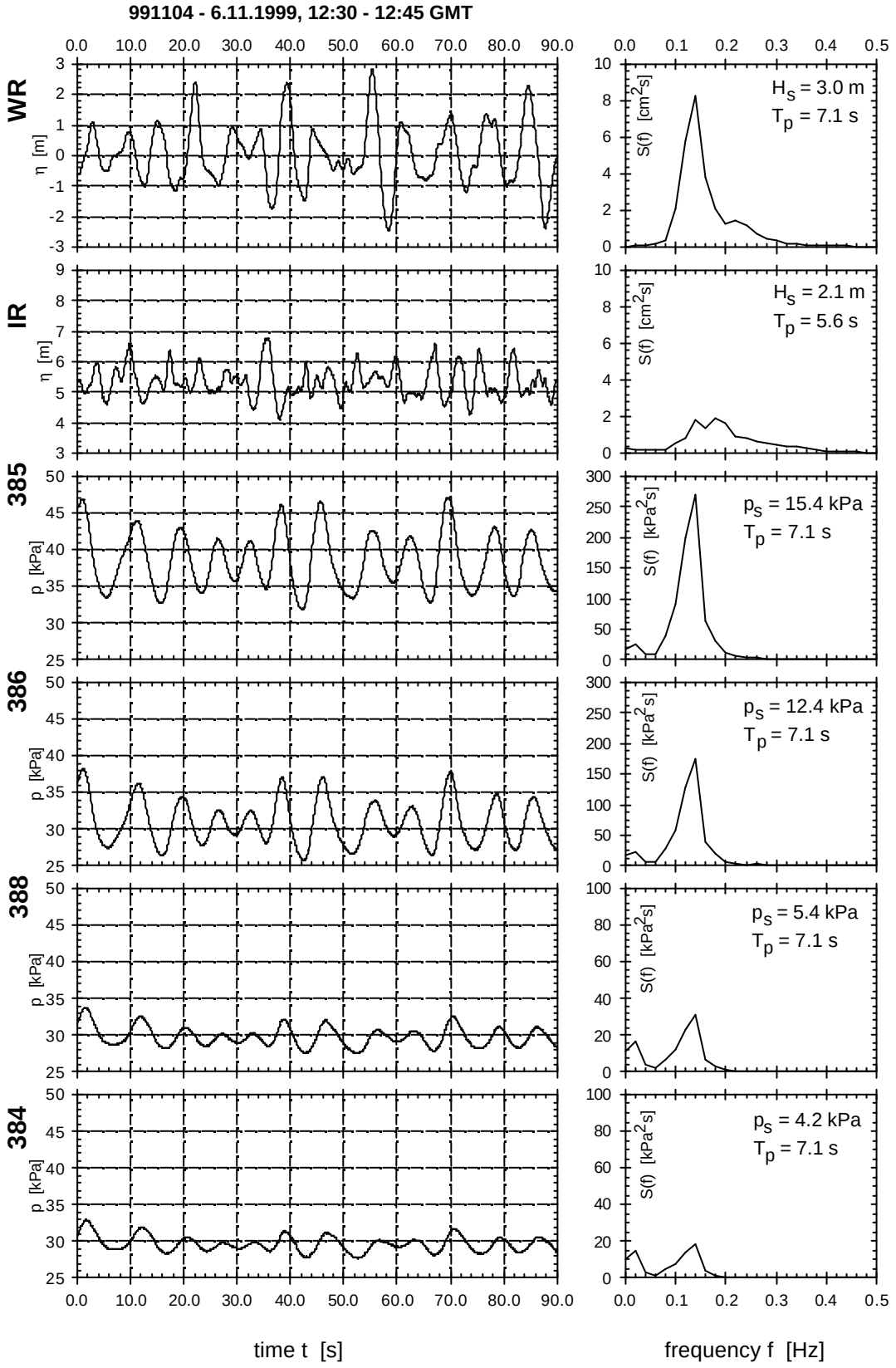

Fig. 4. *Typical prototype time series, and corresponding spectra, of wave buoy WR, IRmeter, and pressure sensors (385, 386, 388, 384) at level Z+2.40, for a 15 minutes wave and pressure record during storm 991104. The attenuation of pore pressure heights inside the core is clearly perceptible in the time series and in the spectrum.*

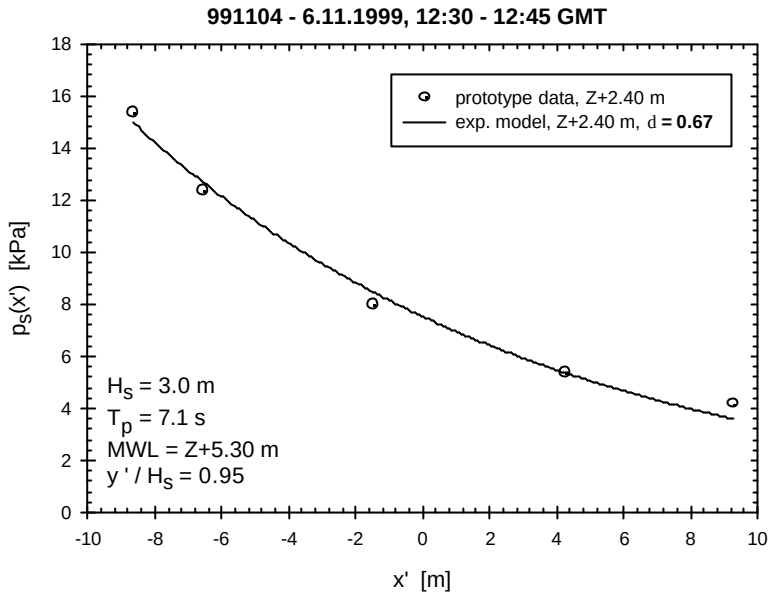

Fig. 5. *Attenuation of prototype pore pressure heights* $p_s(x')$ *and fitting of the damping model (5), for the pressure sensors installed at the level Z+2.40 m, for a 15 minutes pressure record.*

From a more detailed analysis of all prototype storm data (Troch, 2000), the following important conclusions are derived:

- The damping coefficient δ decreases with increasing depth y' between the Mean Water Level (MWL) and the level of pressure sensors.
- The damping coefficient δ decreases with increasing wave steepness.
- There is an interesting relationship between the significant wave height H_s and the significant pore pressure height at the interface between filter layer and core $p_{0,s}$, which is found to be independent of depth y':

$$\frac{p_{0,s}}{\rho_w g} \approx 0.55 H_s \qquad (5)$$

This relationship (5) provides a link (i.e. a constant ratio) between the wave load outside the core and the reference pressure height at the boundary of the core. This also indicates that about 50 % of the energy dissipation already occurs in the armour and filter layers.

2.3 Experimental data from large scale physical model tests

2.3.1 Literature review of physical model tests

Few measurements and results from physical model tests on wave attenuation inside a breakwater core are available in literature, and mostly only qualitative results have been

reported. There is however one comprehensive data set available from large scale physical model tests carried out in the Large Wave Flume (LWF) at Hannover (Germany), as reported by Bürger et al. (1988) and later on by Oumeraci and Partenscky (1990), and in more detail by Oumeraci (1991). The objective of these physical model tests is the experimental study of the evolution of wave induced pore pressures in the core of a typical breakwater on a scale of about 1:5.

Large scale model testing is expensive, requires huge amounts of material, and is both time and labour intensive. However results from large scale testing are very interesting, compared to conventional small scale tests. In large scale models there are no viscous scale effects affecting porous flow inside the core. Compared to prototype data, in large scale model tests there is better control on wave conditions and both material characteristics and geometry are much better known. In the next section the experimental set-up in the LWF and the results reported by Oumeraci and Partenscky (1990) will be briefly described.

2.3.2 Experimental set-up in LWF and reported results

A conventional rubble mound breakwater made of a core, filter and armour layer, has been built in the LWF (Fig. 6). The structure is instrumented with 20 pressure sensors at different horizontal levels throughout the core and in the filter layer. A detailed description of material characteristics and instrumentation is available in Oumeraci (1991).

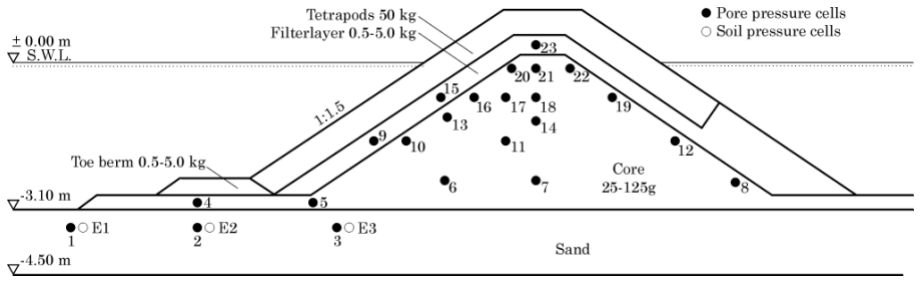

Fig. 6. *Cross section of the tested rubble mound breakwater in the LWF (Hannover, Germany), and location of instruments for pore pressure measurements (source: Oumeraci, 1991).*

Fig. 7 is an example of how the results from the large scale model tests have been reported by Oumeraci (1991). In this case, the distribution of the maximum excess pore pressure heights p_{max} inside the core, in horizontal, vertical and sloping directions is given for irregular waves (T_p = 5.0 s and H_s = 0.40, 0.56 and 0.68 m). The definition "excess pore pressure" refers to the dynamic pore pressure solely induced by wave action, and is equal to zero when no waves are present. The pore pressure height is the height of the time-varying pressure signal (cf. wave height derived from surface elevations) measured by the pressure sensors.

Based on their analysis of the large scale data as presented in Fig. 7, Bürger et al. (1988) and Oumeraci and Partenscky (1990) conclude:

- The largest energy dissipation occurs already in the armour layer and in the filter layer, and the dissipation increases with increasing wave steepness.

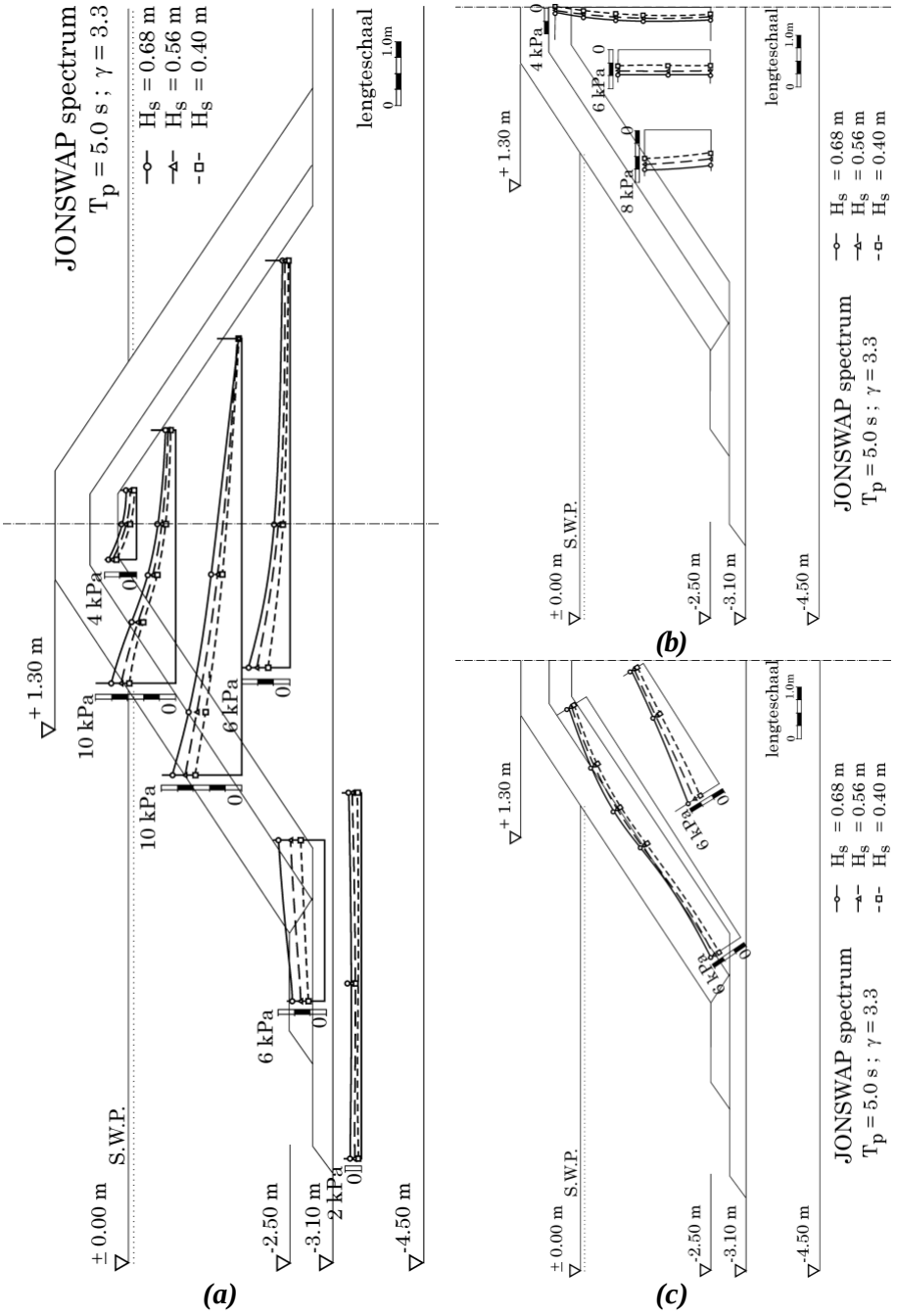

Fig. 7. *Example of reported results from Oumeraci (1991), with (a) horizontal, (b) vertical and (c) sloping distribution of maximum pore pressure height* p_{max} *, for irregular wave attack with* T_p *= 5.0 s and* H_s *= 0.68, 0.56 and 0.40 m resp.*

- The maximum pore pressure heights attenuate exponentially in horizontal direction inside the core, so the damping model (1) may be applicable. The attenuation decreases with increasing distance from the MWL (Fig. 7.a). These observations suggest that the damping coefficient δ is a function of y', the distance between MWL and the horizontal level where the attenuation is considered.

- There is only little attenuation of maximum pore pressure heights in vertical direction (Fig. 7.b).

- The distribution of maximum pore pressure heights along the interface between filter layer and core (and along lines parallel to this interface) is approximately constant (except very close to the MWL). The magnitude of the constant pore pressure heights is dependent on the position of the sloping line inside the core (Fig. 7.c).

Oumeraci and Partenscky (1990) analyse the distribution of the maximum pore pressure heights in the horizontal direction inside the core of the breakwater, using pressure measurements from sensors PC 15 till PC 19 (Fig. 8). The vertical distance y' between MWL and position of sensors is 0.7 m. They present the ratio $p_{max}(x')/p_{0,max}$ versus the non-dimensional distance x'/L' between pressure sensors, where $p_{max}(x')$ is the maximum pore pressure height at position x', and $p_{0,max}$ is the reference pore pressure height from sensor PC 15. Note that PC 15 is located inside the filter layer.

The theoretical model (1) is fitted through the data from all tests, and one global damping coefficient $\delta = 2.0$ is obtained.

From the analysis and the results presented in literature and summarised in this section, it is concluded that only few data on pore pressure attenuation have been reported. Moreover, the analysis of the large scale data set does not include a detailed study of the variation of damping coefficient δ as a function of the wave characteristics and the core material characteristics. Only one global constant value $\delta = 2$ is reported, calculated as average value from all data (see Fig. 8).

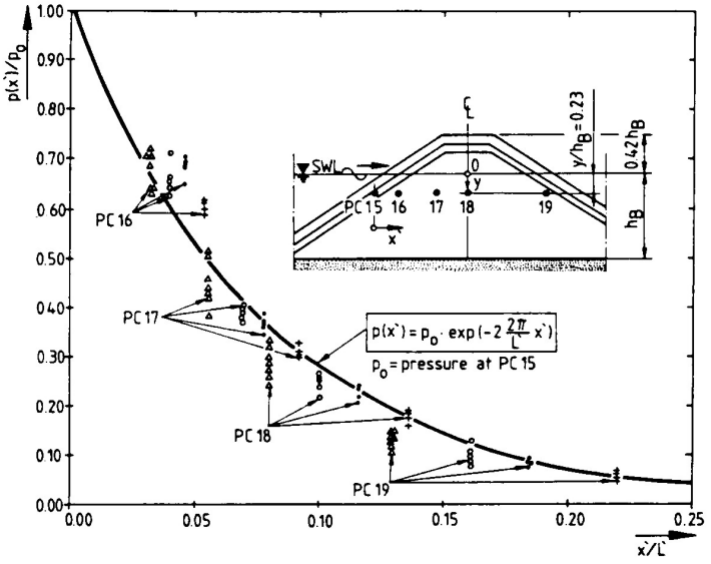

Fig. 8. *Horizontal distribution of maximum pore pressure heights, and fitting of the linear damping model (1) resulting in damping coefficient $\delta = 2.0$ (source: Oumeraci and Partenscky, 1990).*

In the next section, the large scale data set will be re-analysed in more detail with particular attention to the description of the damping coefficient δ as a function of the most important parameters that describe the attenuation of pore pressures inside the breakwater core. When this goal will be achieved, it will be possible to predict the wave attenuation, which would be very useful for other applications, as stated in the introduction.

2.3.3 Analysis of large scale data set

a. Determination of damping coefficient d

Based on Oumeraci's (1991) large scale data set, as presented in Fig. 7, the pore pressure height distributions have been re-analysed for three peak periods T_p = 4.0, 5.0 and 6.0 s, at three depths y' = 0.1, 0.7 and 1.7 m. For each peak period, three significant wave heights H_s have been used. This way, 9 graphs are generated showing the horizontal distribution of the maximum pore pressure heights $p_{max}(x')$ as a function of the parameters y', H_s and T_p. Fig. 9 includes three such graphs, as an example, for T_p = 5.0 s (i.e. for the data presented in Fig. 7).

For each depth y', the damping model (1) is fitted through the data, using the form:

$$p_{max}(x') = p_{0,max} \exp(-\delta \frac{2\pi\sqrt{1.4}}{L_p} x') \qquad (6)$$

The solid lines in the graphs of Fig. 9 indicate the fitted damping model (6). The resulting damping coefficients δ are displayed in the same graphs.

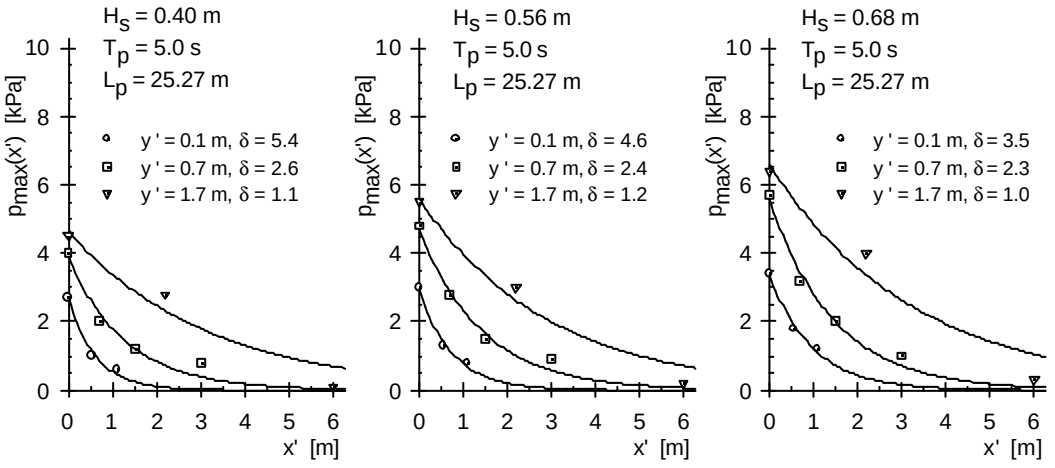

Fig. 9. *Horizontal distribution of maximum pore pressure heights* $p_{max}(x')$ *as a function of the parameters* y' *and* H_s *for* T_p *= 5.0 s (derived from Fig. 7), and fitting of the damping model (1) resulting in damping coefficients* δ.

The resulting damping coefficients δ for all available large scale tests and a detailed analysis of the influence of the parameters y', H_s and T_p on δ are described in Troch (2000). Here the main conclusions will be repeated:

- δ decreases with increasing depth y', for constant wave height H_s and constant wave period T_p;
- δ decreases with increasing wave height H_s, for constant depth y' and constant wave period T_p;
- δ increases with increasing wave period T_p, for constant wave height H_s and constant depth y'.

These conclusions are in agreement with the qualitative conclusions from Oumeraci and Partenscky (1990). However, their average value δ = 2.0 is now described in more detail. The use of a maximum pore pressure height $p_{max}(x')$ is statistically less reliable and less representative than a significant value $p_s(x')$, calculated using (2). Also practical engineering applications will prefer the use of $p_s(x')$ as the significant value in a distribution is a widely used design parameter. The determination of the damping coefficient is invariant with respect to the choice of characteristic pore pressure height: the relative attenuation remains constant. So from here on only the significant pore pressure height $p_s(x')$ will be used. The relationship between maximum pore pressure height and significant pore pressure height is estimated from the assumption that pore pressure heights are Rayleigh distributed (Goda, 1985):

$$p_{max} = \left(\sqrt{\frac{\ln N}{2}} + \frac{0.577}{\sqrt{8 \ln N}} \right) p_s \tag{7}$$

where the number of waves N is around 2000, so equation (7) reduces to

$$p_s = 0.59 p_{max} \tag{8}$$

b. Relationship between wave height and pore pressure height

Again it is possible to propose a relatively simple relationship between the characteristic wave load (i.e. H_s) and the reference pore pressure height at the interface between the filter layer and the core (i.e. $p_{0,s}$). First of all, it provides an estimate of the energy dissipation that occurs in armour and filter layer which is about 50 %. Also the reference pore pressure height is the starting point for the determination of the attenuation of the pore pressures inside the core of the breakwater. The observation that the pore pressure height $p_{0,s}$ is constant along the interface makes this relationship with H_s very simple. From a detailed analysis of the large scale data set, Troch (2000) proposes for practical applications:

$$\frac{p_{0,s}}{\rho_w g} \approx 0.55 H_s \tag{9}$$

c. Simple expression for damping coefficient d

Based on the results from the extended analysis of the large scale data and based on the conclusions from Fig. 9, an expression for the damping coefficient δ as a function of the most important parameters H_s and T_p (wave conditions), y' (position in core) and porosity n (core material characteristics) is developed (Burcharth, Liu and Troch, 1999). The proposed expression for δ is:

$$\delta = a_\delta \frac{n^{\frac{1}{2}} L_p^2}{H_s b} \tag{10}$$

From this linear relationship (10) between the damping coefficient δ and the non-dimensional parameter $n^{\frac{1}{2}} L_p^2 / H_s b$, it follows that δ increases :

- with increasing porosity n of the core material (rock);
- with increasing wave period T_p (included in L_p);
- with decreasing wave height H_s;
- with decreasing width b of the core at depth y' below MWL.

Fig. 10 shows the fitting of the linear relationship (10) to all damping coefficients δ derived from the large scale data set, from where the slope a_δ is obtained as (Troch, 2000):

$$a_\delta = 0.0140 \tag{11}$$

Good agreement is observed, especially for smaller δ - values. For higher δ - values ($\delta > 3.0$) the deviation increases. However these data points are derived from pressure measurements at the depth y' = 0.1 m which is too close to the MWL for accurate pressure measurements. Indeed the pressure waves that propagate into the breakwater core are too much influenced by the vicinity of the free water surface. It is therefor better not to use these δ - values higher than 3. These will be disregarded in the subsequent analysis.

2.4 Development of calculation method for pore pressure attenuation

2.4.1 Comparison between prototype data and large scale data

Based on the analysis in previous sections and the subsequent results of Zeebrugge prototype data and large scale data, a calculation method for the attenuation of pore pressure heights will be developed here. First a comparison between the results of the experimental study from both data sets is made:

- The theoretical exponential damping model (1) is valid for both data sets, and corresponding damping coefficients δ have been obtained by fitting (1) to the data sets.

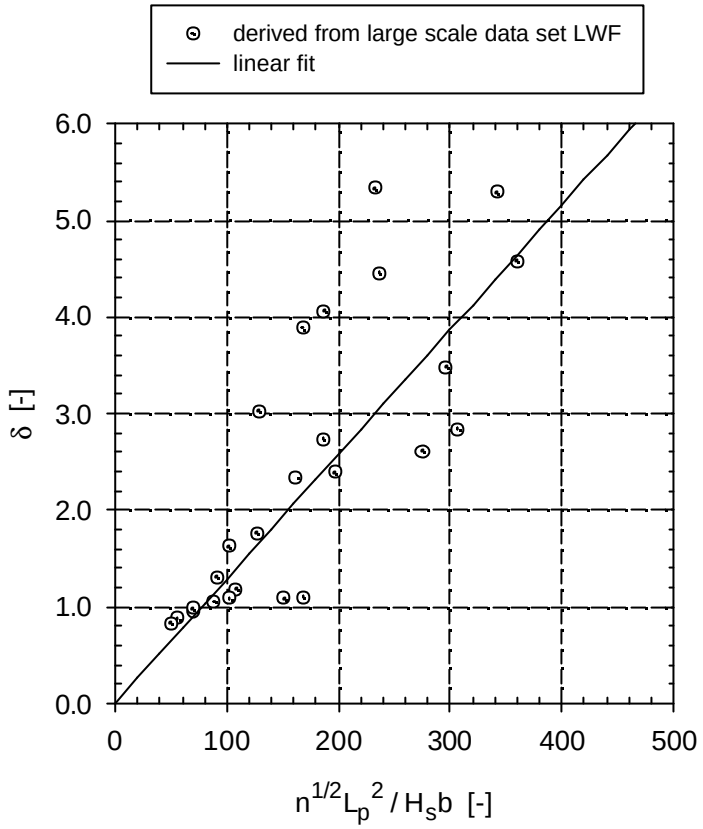

Fig. 10. *Derivation of linear relationship (10) between damping coefficient* δ *and the four parameters wave height* H_s, *wave period* T_p, *depth* y' *and porosity* n, *based on the large scale data set from LWF.*

- The constant relationship (5) or (9) holds for both data sets, and is based on the observation that the reference pore pressure height is constant along the interface between filter layer and core: $p_{0,s} \approx \text{cte}$.

- A simple expression (10) for the damping coefficient δ is obtained from fitting through the large scale data. When using both the large scale data (rejecting δ- values > 3.0) and the prototype data for the determination of the slope of the expression (10), a linear fitting yields (Fig. 11):

$$a_\delta = 0.0123 \qquad (12)$$

From Fig. 11 it is concluded that there is a good agreement between the large scale LWF data set, the Zeebrugge prototype data set and the linear relationship (10). Due to the inclusion of the prototype data and the rejection of damping coefficients δ > 3.0 (this corresponds to the criterion $y'/H_s < 0.85$), the slope decreases slightly from $a_\delta = 0.0140$ down to $a_\delta = 0.0123$. The range of the data points on both axes is much smaller for the prototype data than for the large scale physical model data. This means that the prototype data are usable for validation or verification purposes rather than for detailed parametric analysis. In a physical model it is much easier to obtain the total range of wave parameters simply by adjusting the wave paddle and the water depth.

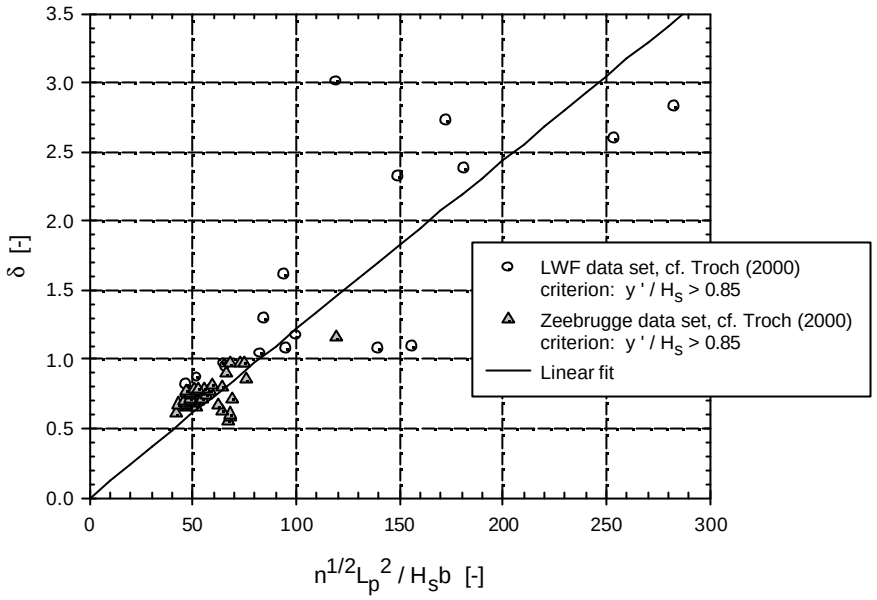

Fig. 11. *Derivation of linear relationship (10) between damping coefficient* δ *and the four parameters* H_s, T_p, y' *and* n, *based on the large scale data set from LWF and on the Zeebrugge prototype data set.*

2.4.2 Calculation method for the attenuation of pore pressure heights inside a rubble mound breakwater core

The conclusions from the experimental study of both data sets are synthesised into a relatively simple but practical and reliable calculation method. This method predicts the distribution and attenuation of the pore pressures at each location inside the core of a rubble mound breakwater, and is based on a limited number of input parameters. These four input parameters are considered to be the most important parameters influencing the pore pressures. Moreover these are easy to estimate during the design process.

The consecutive steps of the calculation method are listed here and are presented in Fig. 12.

- First the wave climate is determined, i.e. the significant wave height H_s and the peak wave period T_p in water depth d in front of the breakwater. The wave length L_p is calculated using the dispersion relationship from linear wave theory.

- Due to the considerable energy dissipation that occurs in armour and filter layers, only about 55 % of wave energy arrives at the interface between filter layer and core. Moreover the pore pressure height along the interface $p_{0,s}$ is constant and not dependent on y'. These conclusions are represented by using the expressions $\frac{p_{0,s}}{\rho_w g} \approx 0.55 H_s$ (9), and $p_{0,s} \approx cte$.

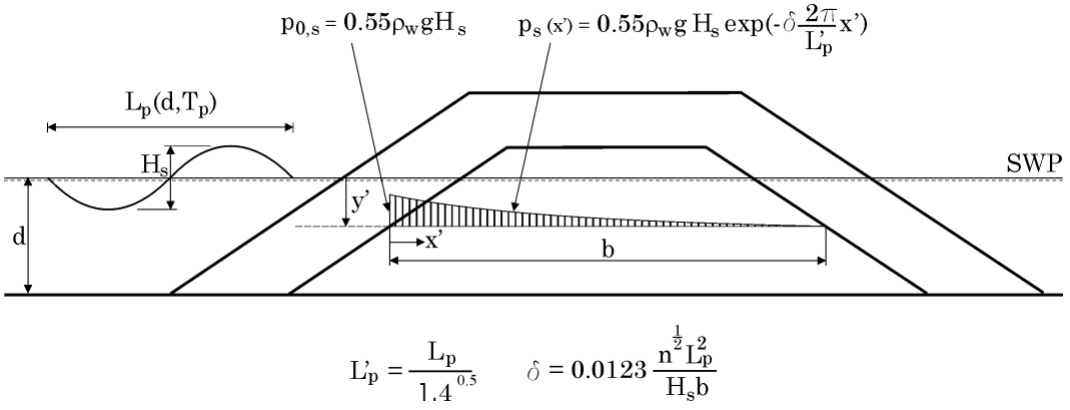

Fig. 12. *Definition sketch for the proposed calculation method for the determination of the distribution and attenuation of pore pressure heights inside a rubble mound breakwater core.*

- The attenuation of the pore pressure heights in horizontal direction is expressed by the exponential damping model $p_s(x') = p_{0,s} \exp(-\delta \frac{2\pi}{L'} x')$ (4), and the damping coefficient that has to be used is calculated from the simple expression $\delta = a_\delta \frac{n^{\frac{1}{2}} L_p^2}{H_s\, b}$ (10), where a_δ = 0.0123 (12).

The calculation method is not applicable in areas where $y'/H_s < 0.85$ due to the presence of the free surface. The calculation method does not take into account the phreatic set-up of the internal water table neither the hydrostatic pressure.

The proposed calculation method is very useful in applications where the knowledge of the pore pressure distribution is important, such as in the slope stability analysis. Another new application that becomes available, is the distorted scaling of the breakwater core in a small scale physical model test in order to reduce viscous scale effects. This new scaling method is based on Froude scaling of flow fields rather than of length scales, and makes use of the expected pore pressure distribution in the core (Burcharth, Liu and Troch, 1999). The new scaling method is an improvement of the well-known Juul Jensen and Klinting scale distortion method (1983).

3 Numerical modelling of pore pressure attenuation

3.1 Development of a numerical wave flume VOFbreak[2]

In the previous sections the attenuation of the pore pressures inside a rubble mound breakwater have been studied experimentally using prototype data and large scale physical model data. Another tool to study this phenomenon is the numerical modelling of the wave interaction with the breakwater. Such a numerical study of the wave interaction and the induced pore pressures is also carried out. The main results with respect to the pore pressure

attenuation inside the breakwater core will be described here and will be compared to the results from the experimental study.

The numerical modelling is carried out using a numerical wave flume, called VOFbreak^2 (Troch, 1997). It is based on the original SOLA-VOF code capable to compute free surface flow when the fluid domain becomes multiply connected (Hirt and Nichols, 1980). Incompressible Newtonian fluid with uniform density is assumed in the vertical plane (two dimensional), governed by the Navier-Stokes equations and the continuity equation. The Volume Of Fluid (VOF) method is used for the treatment of the free surface configuration. Finite difference solutions are obtained on an Eulerian rectangular mesh in Cartesian geometries.

A number of modifications have been implemented into the original code in order to allow the simulation of the wave interaction with a rubble mound breakwater:

- Porous Flow Model: The governing Navier-Stokes equations are extended, to include the simulation of porous flow inside the permeable core of the breakwater, using Forchheimer flow resistance terms.

- Wave Boundary Conditions: A number of wave boundary conditions are implemented. Incident waves are generated using boundary wave generation. Linear wave theory is applied at the boundary of the computational domain to provide the surface elevation and the velocity components of the incident wave at the boundary. For absorption at the boundary of reflected waves, the active wave absorbing technique AWAVOF is used (Troch and De Rouck, 1999). This new numerical boundary condition is based on an active wave absorption system that is well known already for physical wave flume application using a wave paddle. Velocities are measured at one location inside the computational domain. The reflected wave train is separated from the wave field in front of the structure by means of digital filtering and subsequent superposition of the measured velocity signals. This way an additional incident wave train is determined in order to absorb the reflected wave train. The AWAVOF method is optimised for efficient use in a numerical wave flume and applies to regular and irregular waves.

- Code Portability: The code is implemented using ANSI C, providing general computer compatibility, and providing a flexible code structure for adaptations with little effort. A series of post-processing tools has been developed, using Tcl/Tk for the visualisation, processing and interpretation of the computed results. Numerical instrumentation for the acquisition of relevant phenomena (wave height, run-up level, pore pressure, surface elevation, ...) is included for easy access to calculated data.

These modifications allow the numerical modelling of the wave induced pore pressure attenuation inside a breakwater core. The detailed description of the theoretical background and the implementation of the modifications are reported in Troch (2000). Before the numerical simulation of the wave interaction is started, a detailed validation process has to be carried out using physical model data. The results from this validation are described briefly in the next section.

3.2 Validation of numerical wave flume using physical model tests

Physical model test data have been acquired in a wave flume at Aalborg University (Denmark) in 1997 for the validation of the wave interaction with a breakwater. The test set-up included a relatively simple breakwater lay-out with a vertical front wall and a core of homogeneous rock (porosity $n = 0.426$, mean grain size $d_{50} = 0.0181$ m), Fig. 13.

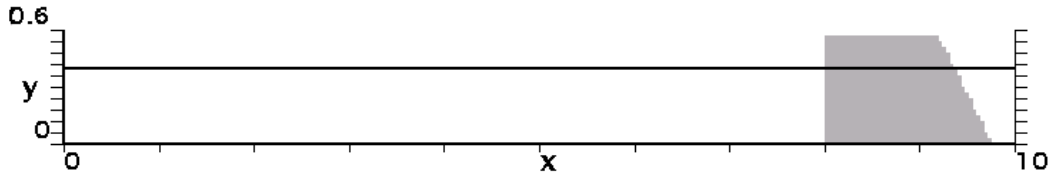

Fig. 13. *Geometry of the wave flume set-up, with wave generation and absorption at the left boundary (x = 0) and the breakwater near the right boundary.*

The validation process aims at comparing the reflection, run-up, transmission and pore pressures from both the physical model and the numerically simulated equivalent model for the same geometry, material characteristics and wave conditions. In this section, only a comparison with respect to the pore pressures will be discussed. A comparison for the other processes is available in Troch (2000).

The numerically calculated pore pressures inside the core are compared with the pore pressure measurements from the physical model at five positions on two horizontal levels. Fig. 14 shows an example of the validation results for one test (reg10h), at two horizontal levels y' resp., for incident regular waves ($H = 0.06$ m, $T = 1.80$ s). In this case the viscous friction term is neglected and only turbulent friction losses are accounted for in the Forchheimer porous flow resistance model.

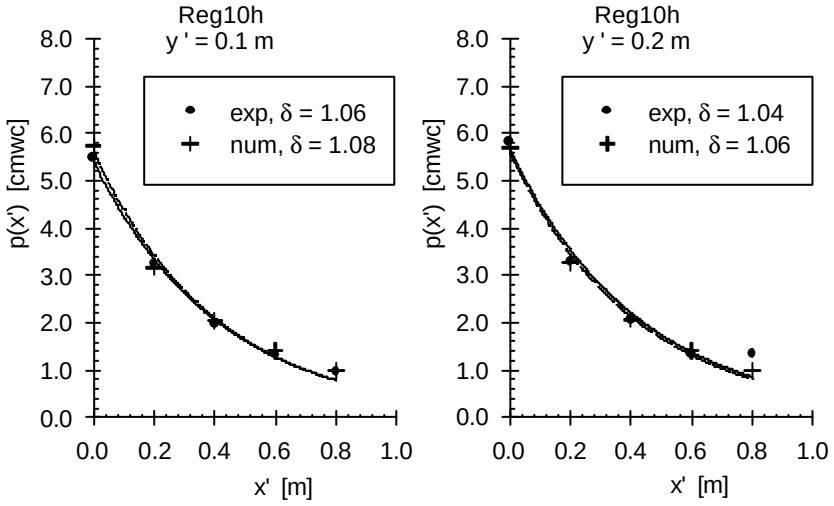

Fig. 14. *Distribution of pore pressure heights* $p(x')$ *versus position* x'*, for two levels at resp. depth* $y' = 0.10$ *m and* $y' = 0.20$ *m, calculated from physical model tests (exp) and numerical simulations (num) resp., for test reg10h.*

The solid and dashed lines in Fig. 14 indicate the fitted exponential damping model (1) through the experimental and the numerical data resp., from where the damping coefficient δ is obtained and plotted in Fig. 14. It is clear from Fig. 14 that very good agreement is found between the physical model test data and the numerically calculated data.

From these results (in fact from a much more detailed validation analysis, see Troch, 2000) it is concluded that the numerical model VOFbreak^2 is capable of simulating the wave interaction with a simple breakwater.

3.3 Numerical modelling of wave interaction with breakwater

Finally a breakwater with a more conventional geometry will be used for a numerical modelling of the wave interaction. The resulting pore pressures will be analysed and compared to the results from the experimental analysis.

The Zeebrugge prototype breakwater is tested in the numerical wave flume VOFbreak^2. A number of approximations have been used. The bathymetry in front of the breakwater is simplified by using a constant water depth d = 8.0 m. The incident waves are regular waves with wave height H = 3.0 m and wave period T = 8.0 s. The AWAVOF wave absorption system is switched on. The considerable energy dissipation in the armour and filter layers is modelled by using a layer on top of the breakwater core with higher permeability than the core material.

Fig. 15 shows the numerical set-up with the wave generation/absorption system AWAVOF at the left boundary (x = 0 m) and the Zeebrugge breakwater with simplified geometry near the other boundary. At the right boundary (x = 160 m) a passive wave absorption system is installed. The simulation is started from still water conditions.

The cell dimensions are Δx = 0.50 m and Δy = 0.40 m in x and y-direction resp., resulting in 323 x 43 cells for the complete computational domain. The total simulation time is set to 200 s with a time step of Δt = 0.005 s. The calculations took 4 hours on a Pentium III PC.

Fig. 16 shows the resulting free surface position in front of the breakwater, in the armour layer and in the core from the simulation at t = 122 s (run-down) and t = 127 s(run-up). Inside the armour layer the energy dissipation of the wave action and the damped movements of the free surface are observed. The variation of the water level in the core is even more attenuated resembling the working principle of a breakwater.

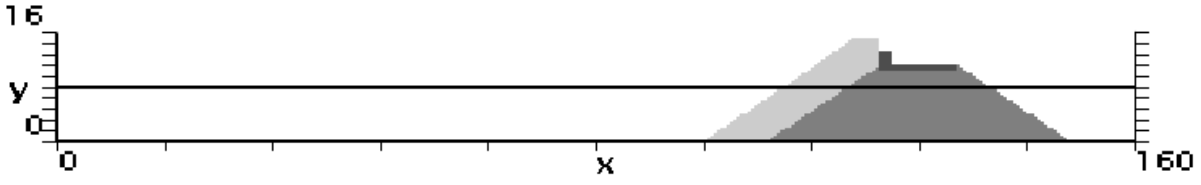

Fig. 15. *Geometry of the numerical wave flume set-up, with wave generation and absorption at the left boundary (x = 0) and the simplified Zeebrugge breakwater near the right boundary (non-distorted scales).*

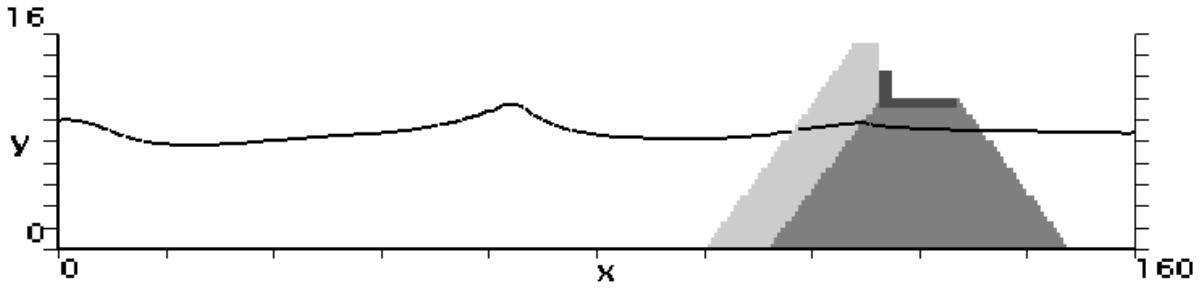

(a) wave run-up at t = 122 s

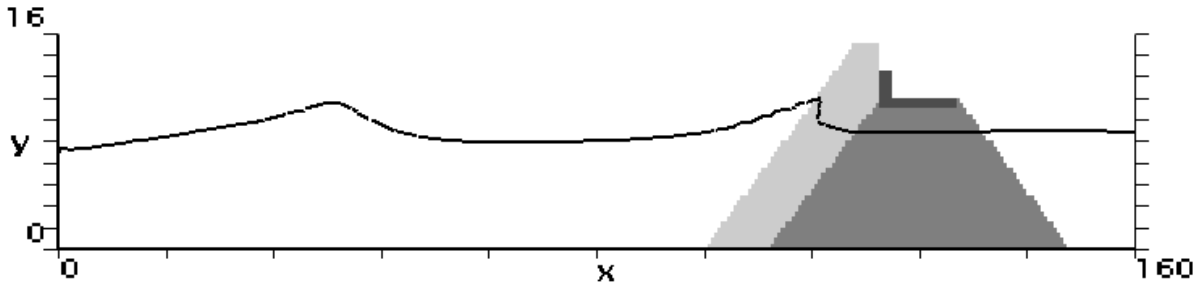

(b) wave run-down at t = 127 s

Fig. 16. *Results from numerical simulation with Zeebrugge breakwater at t = 122 s and t = 127 s, showing the free surface in front of the breakwater, in the armour layer and in the core (distorted scale in y direction using factor 2).*

In Fig. 16 only information from the time instant of the two 'snap-shots' is available. It is relatively easy to visualise the numerical results during a complete wave period in order to increase the information that is calculated. In Fig. 17 the results from the calculations (pressure p, and velocity components u and v) are given for a cycle of one wave period. Instantaneous values at t = (i/9)T (i = 1, 2, ..., 8) and envelope values of pressure and velocities along the x-axis are presented. The data are taken from the horizontal level located one wave height below the still water level, and are given for the foreshore area (left column) and for the breakwater area (right column). In the graphs of the right column, the x-axis has been stretched for better visualisation. Also, the u- and v-axis in the right column have been stretched (factor 2) for better visualisation. The hatched area is the area inside the armour layer.

From these graphs in Fig. 17 it is seen that both pressure and velocities attenuate inside the armour layer and even more in the breakwater core. This physical behaviour is comparable to the prototype processes. The pore pressure amplitudes decrease exponentially towards the backward slope where the pore pressure is almost zero. Maximum velocities (both u and v) inside the core are about 0.25 m/s close to the slope and decrease gradually to 0 m/s near the backward slope. The horizontal velocity u in the volume of water running up and down the slope is about two times higher than the vertical velocity at the same location. This indicates that infiltration and seepage processes predominantly act in horizontal direction.

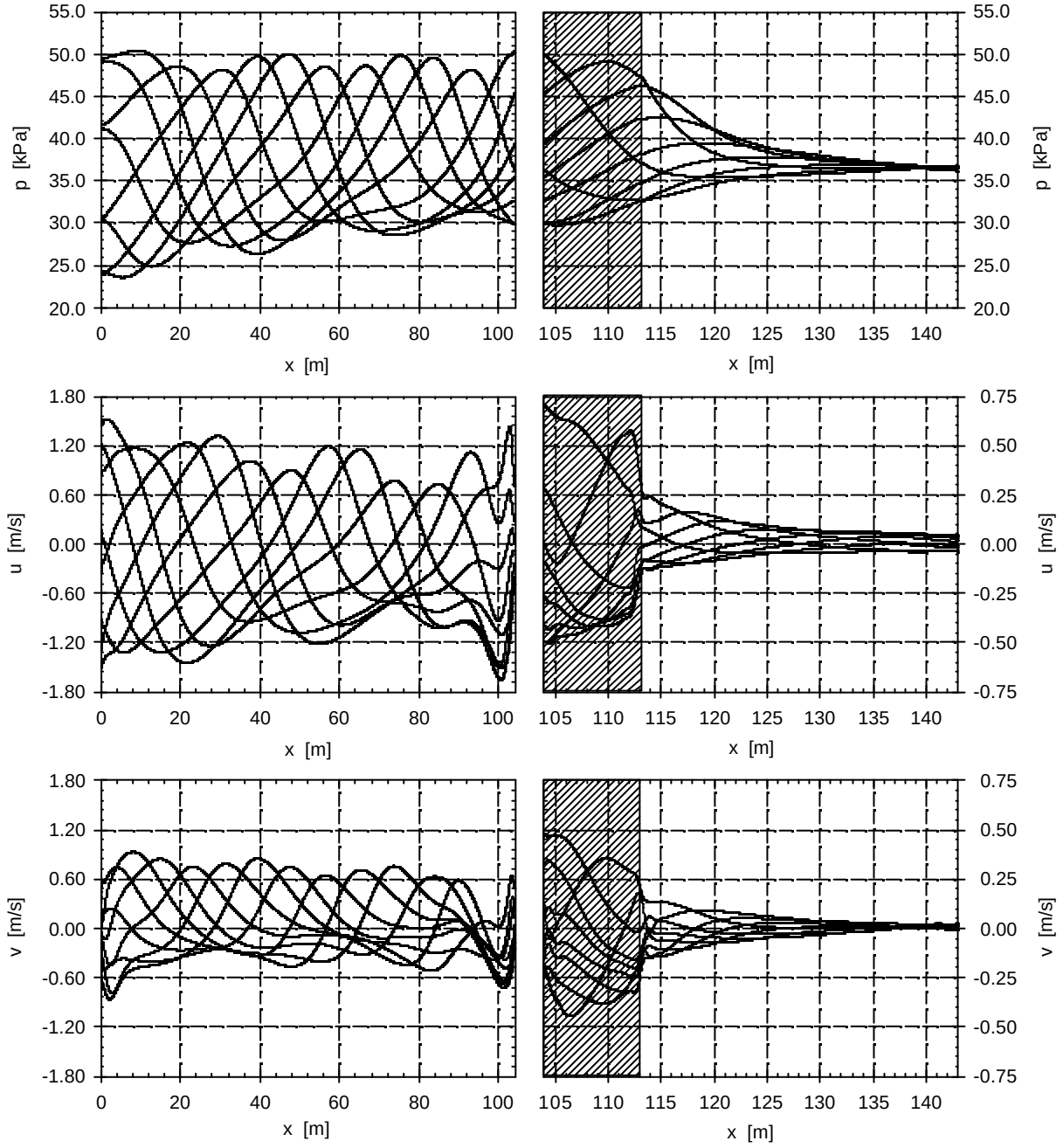

Fig. 17. *Calculated instantaneous values of pressure p and velocities u, v (and envelopes) vs. position x located one wave height below the still water level, for 8 consecutive time instants during one wave period between t = 120 s and t = 127 s. Left column is for the foreshore area (water), right column is for the breakwater area (armour layer - hatched area- and core material).*

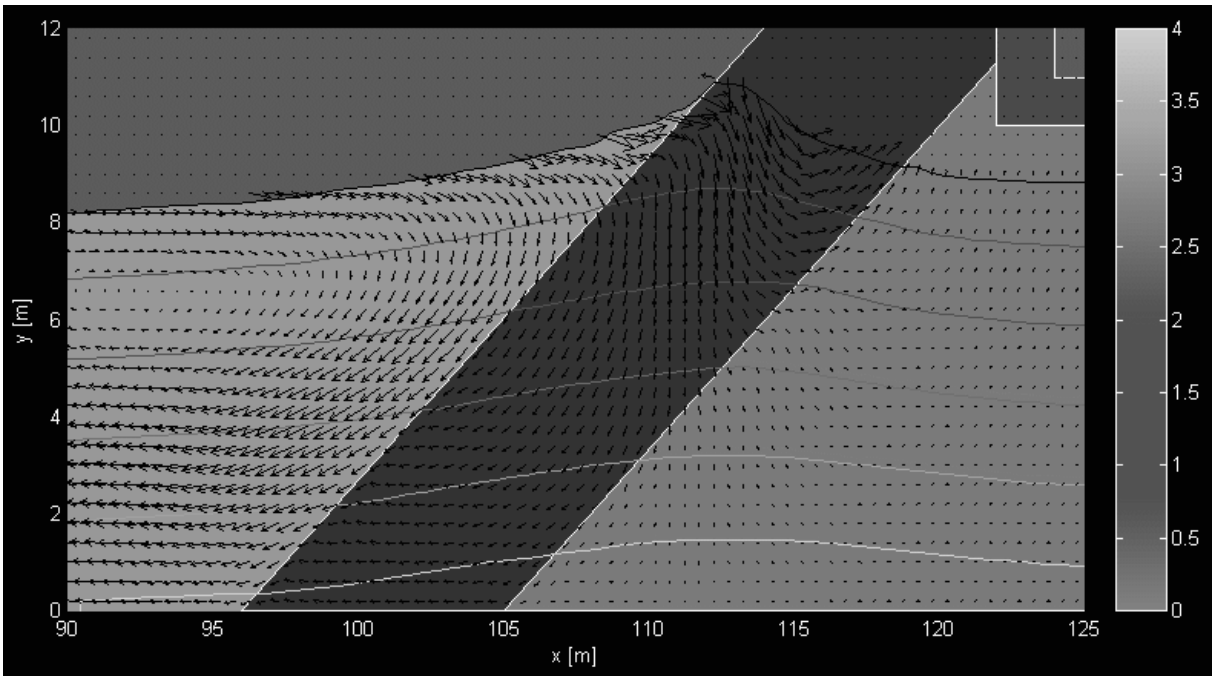

Fig. 18. *Zoom of calculated flow field near the breakwater slope during wave run-up at t = 127 s.*

Finally in Fig. 18 a snap-shot of the detailed calculated flow field in the zoomed area around the breakwater slope is given for the case of wave run-up at t = 127 s. Fig. 18 shows the velocity vector field, the isobars and the position of the free surface. It is clearly perceptible that during wave run-up both infiltration (near the free surface) and seepage (near the bottom) occur at the same time along the slope. The wave interaction therefor cannot be reduced to one dimension.

3.4 Comparison between experimental results and numerical simulations

In the previous section pore pressures have been calculated numerically for the case of the Zeebrugge breakwater. It is straightforward and very interesting to compare the results from the numerically obtained pore pressures with the results from the experimental study. Therefor the pore pressures have been analysed at three horizontal levels below the Still Water Level (SWL), at five locations in the core and at two locations in the armour layer at a time. Fig. 19 shows the result of the analysis. The pore pressure heights $p(x)$ have been plotted versus the horizontal distance x. When comparing the numerical results with the results from the prototype data in section 2, it is concluded from Fig. 19:

- The reference pore pressure heights along the interface between armour layer and core are more or less constant: $p_0 \approx \text{cte}$.

- The constant ratio between reference pore pressure height and incident wave height, i.e. $p_0/\rho_w gH = 0.50$, is comparable to (5).

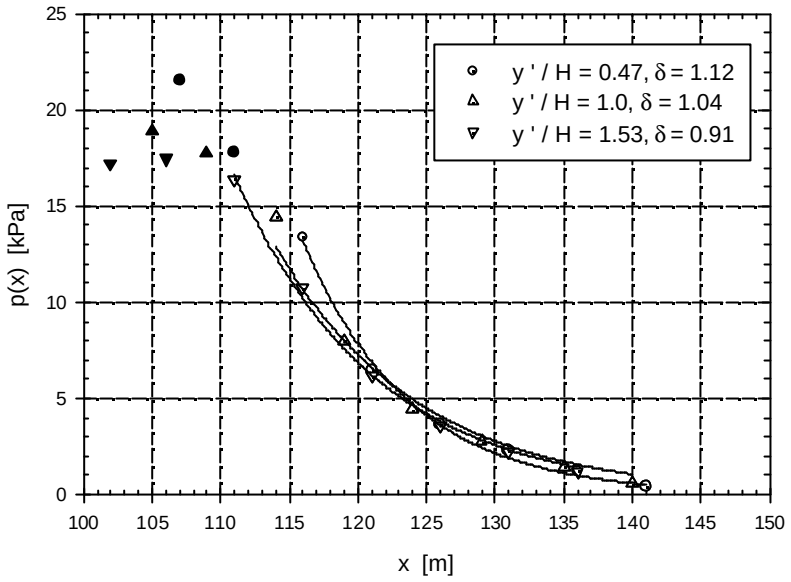

Fig. 19. *Pore pressure attenuation inside the armour layer (black symbols) and inside the core (white symbols) of the breakwater obtained from the numerical simulations, and fitted exponential damping model (1).*

- From the fitted damping model (1) through the numerical pore pressure heights, damping coefficients δ are obtained and plotted in Fig. 19. It is concluded again that the damping coefficient decreases with increasing distance below SWL.

4 Conclusions

The attenuation of the wave induced pore pressures inside the core of a rubble mound breakwater has been studied experimentally and numerically. The exact knowledge of the distribution of the pore pressures is very important for the design of a stable and safe breakwater structure.

Based on a theoretical background, an exponential damping model is derived for the attenuation of the pore pressure height inside the breakwater core. The attenuation is governed by a damping coefficient δ.

The experimental study has been based on two data sets. The prototype data have been acquired at the Zeebrugge breakwater. The prototype monitoring system has been described with respect to its infrastructure, instrumentation and data management. From the analysis of the prototype data, it is concluded that the theoretical damping model fits well, and damping coefficients have been obtained.

The large scale physical model data, taken from literature, have been re-analysed in detail. Again good agreement with the theoretical damping model has been found, and damping coefficients have been obtained.

When comparing the prototype data and the large scale data, a number of important conclusions have been made that are common to both data sets. There is a constant relationship between the incident wave height and the reference pore pressure height at the interface between the filter layer and the breakwater core. Moreover the reference pore pressure height is constant along the interface. Finally a simple linear expression is derived for determination of the damping coefficient δ as a function of the four most important parameters depth y', wave height H_s, wave period T_p and porosity n of the core material.

Based on the experimental study, a calculation method has been proposed for the determination of the attenuation of the pore pressure heights inside the breakwater core. The consecutive steps have been presented in detail. The calculation method will be very useful for applications where information about the pore pressure distribution or the porous flow velocities is required, such as slope stability analysis or a new scaling method for physical small scale models.

The pore pressure attenuation has been studied in the numerical wave flume VOFbreak^2. The successful validation of the wave interaction with a breakwater has been presented. The Zeebrugge breakwater with simplified geometry has been modelled in the numerical wave flume. From analysis of the numerically obtained pore pressures and comparing to the experimentally obtained conclusions, the same conclusions on the pore pressure distribution have been found.

The work presented in this paper is a combination of theoretical, experimental and numerical work in order to study the wave induced pore pressures in the breakwater core. Hopefully it will be a clear contribution to the design tools related to rubble mound structures.

Acknowledgements

The development of the Ph.D. work originated during the EC MAST2 project MAS02-CT92-0023, and continued in the EC MAST3 project OPTICREST MAS3-CT97-0116. The financial support of EC is greatly acknowledged.

The author is grateful to the project partners of OPTICREST for fruitful discussions and comments during meetings and workshops, and especially to prof. H.F. Burcharth for permission to perform physical model tests in the wave flume at Aalborg University (Denmark).

The author wishes to thank ir. B. De Putter and ir. L. Van Damme from Coastal Division of Ministry of Flemish Community (Belgium), as owner of the prototype monitoring system, for the permission to use and publish the results from the Zeebrugge prototype data and for the continuous interest and assistance in the development of the research on the prototype monitoring system.

The detailed report on the large scale physical model data in the Large Wave Flume has been provided by prof. H. Oumeraci from Leichtweiss Institut für Wasserbau (Braunschweig, Germany).

Finally, the author wishes to thank the promotor of his Ph.D. thesis, prof. J. De Rouck (Ghent University, Belgium), for his support and encouragement during the research work.

REFERENCES

Allsop N.W.H.., Wood L.A., 1987. Hydro-geotechnical performance of rubble mound breakwaters. Hydraulics Research Report SR 98 (UK).

Barends F.B.J., 1986. Geotechnical aspects of rubble mound breakwaters. Proc. Breakwaters '86, London, Thomas Telford (UK).

Biésel F., 1950. Equations de l'écoulement non lent en milieu perméable. La Houille Blanche, No. 2.

Burcharth H.F., Andersen O.H., 1995. On the one-dimensional steady and unsteady porous flow equations. Coastal Engineering, Vol. 24, pp 233-257, Elsevier.

Burcharth H.F., Liu Z., Troch P., 1999. Scaling of core material in rubble mound breakwater model tests. Proc. 5th COPEDEC, Cape Town (South Africa), pp. 1518-1528.

Bürger W., Oumeraci H., Partenscky H.W. 1988. Geohydraulic investigations of rubble mound breakwaters. Proc. 21th ICCE Malaga.

de Groot M.B., Yamazaki H., van Gent M.R.A., Kheyruri Z., 1994. Pore pressures in rubble mound breakwaters. Proc. 24th Int. Conference on Coastal Engineering, Kobe, Japan. ASCE, New York, Vol. 2, pp 1727-1738.

Goda Y., 1985. Random seas and desing of marine structures. University of Tokyo Press, Japan.

Harlow E.H., 1980. Large rubble mound breakwater failures. Proc. ASCE Jo. W'way, Port and Coastal Div., Vol. 106, WW2.

Hirt C.W., Nichols B.D., 1981. J. Comp. Phys. Vol. 39, pp. 201-225.

Juul Jensen O., Klinting P., 1986. Evaluation of scale effects in hydraulic models by analysis of laminar and turbulent effects. Coastal Engineering Vol. 7, pp. 319-329.

Le Méhauté, B., 1958. Perméabilité des digues en enrochements aux ondes de gravité periodiques. La Houille Blanche No. 6, 1957 et No. 2, 3, 1958.

Oumeraci H., 1991. Wave induced pore pressures in a rubble mound breakwater. Internal Technical Report LWI, Technical University Braunschweig, Germany.

Oumeraci H., Partenscky H.W., 1990. Wave-induced pore pressures in rubble mound breakwaters. Proc. 22th International Conference on Coastal Engineering.

Price W.A., 1983. Some thoughts on the future design of breakwaters. Keynote lecture of Proc. of Coastal Structures '83, ASCE.

Thornton et al., 2000. State of nearshore processes research: part II. Technical report NPS-OC-00-001, Naval Postgraduate School, California, USA.

Troch P. Experimental study and numerical simulation of wave interaction with rubble mound breakwaters. Ph.D. thesis, Dept. Of Civil Engineering, Ghent University, Belgium, (2000).

Troch P., De Somer M., De Rouck J., Van Damme L., Vermeir D., 1996-a. In situ load monitoring of rubble mound breakwaters. Proc. 11th Int. Harbour Congress, 17-21 June 1996, Antwerp (Belgium), pp. 331-341.

Troch P., De Somer M., De Rouck J., Van Damme L., Vermeir D., Martens J.P., Van Hove C., 1996-b. Wave attenuation inside a rubble mound breakwater based on full scale measurements. Proc. 25th Int. Conference on Coastal Engineering, Orlando, USA.

Troch P., De Rouck J., Van Damme L., 1998. Instrumentation and prototype measurements at the Zeebrugge rubble mound breakwater. Coastal Engineering, Vol. 35 (1-2), pp. 141-166.

Troch P., De Rouck J., 1999. An active wave generating-absorbing boundary condition for VOF type numerical model. Coastal Engineering, Vol. 38 (4), pp. 223-247.